www.elsevier.com/locate/developmentalbiology

Evolution of the developmental plasticity and a coupling between left mechanosensory neuromasts and an adaptive foraging behavior

Vânia Filipa Lima Fernandes, Christian Macaspac, Louise Lu, Masato Yoshizawa

PII: S0012-1606(18)30118-0
DOI: https://doi.org/10.1016/j.ydbio.2018.05.012
Reference: YDBIO7768

To appear in: *Developmental Biology*

Received date: 13 February 2018
Revised date: 10 May 2018
Accepted date: 15 May 2018

Cite this article as: Vânia Filipa Lima Fernandes, Christian Macaspac, Louise Lu and Masato Yoshizawa, Evolution of the developmental plasticity and a coupling between left mechanosensory neuromasts and an adaptive foraging behavior, *Developmental Biology,* https://doi.org/10.1016/j.ydbio.2018.05.012

Evolution of the developmental plasticity and a coupling between left mechanosensory neuromasts and an adaptive foraging behavior

Vânia Filipa Lima Fernandes, Christian Macaspac, Louise Lu and Masato Yoshizawa*

Department of Biology, University of Hawai‘i at Mānoa, Honolulu, HI 96822, USA.

Correspondence to: Department of Biology, University of Hawai‘i at Mānoa, 2538 McCarthy Mall, Honolulu, HI 96822, USA. Email address: yoshizaw@hawaii.edu (M. Yoshizawa)

Abstract

Many animal species exhibit laterality in sensation and behavioral responses, namely, the preference for using either the left or right side of the sensory system. For example, some fish use their left eye when observing social stimuli, whereas they use their right eye to observe novel objects. However, it is largely unknown whether such laterality in sensory-behavior coupling evolves during rapid adaptation processes. Here, in the Mexican tetra, *Astyanax mexicanus*, we investigate the laterality in the relationship between an evolved adaptive behavior, vibration attraction behavior (VAB), and its main sensors, mechanosensory neuromasts. *A. mexicanus* has a surface-dwelling form and cave-dwelling forms (cavefish), whereby a surface fish ancestor colonized the new environment of a cave, eventually evolving cave-type morphologies such as increased numbers of neuromasts at the cranium. These neuromasts are known to regulate VAB, and it is known that, in teleosts, the budding (increasing) process of neuromasts is accompanied with dermal bone formation. This bone formation is largely regulated by endothelin signaling. To assess the evolutionary relationship between bone formation, neuromast budding, and VAB, we treated 1-3 month old juvenile fish with endothelin receptor antagonists. This treatment significantly increased cranial neuromasts in both surface and cavefish, and the effect was significantly more pronounced in cavefish. Antagonist treatment also increased the size of dermal bones in cavefish, but neuromast enhancement was observed earlier than dermal bone formation, suggesting that endothelin signaling may independently regulate neuromast development and bone formation. In addition, although we did not detect a major change in VAB level under this antagonist treatment, cavefish did show a positive correlation of VAB with the number of neuromasts on their left side but not their right. This laterality in correlation was observed when VAB emerged during cavefish development, but it was not seen in surface fish under any conditions tested, suggesting this laterality emerged through an evolutionary process. Above all, cavefish showed higher developmental plasticity in neuromast number and bone formation, and they showed an asymmetric correlation between the number of left-right neuromasts and VAB.

Keywords

Endothelin, ET, neuromast, lateral line, adaptation, laterality, flow dynamics, foraging, prey location

1. Introduction

Many animals show laterality, a preference for the right or left side, when using sensory systems such as the eyes (Bisazza et al., 1998; Rogers and Andrew, 2002; Vallortigara and Bisazza, 2002) and, in some fishes, when using the mechanosensory lateral line (Perera and Braithwaite, 2005). Lateralization is thought to offer advantages in performing complex motor activities (Magat and Brown, 2009), spatial learning (Sovrano et al., 2005), recognizing predators (Chivers et al., 2017) and escaping predators (Chivers et al., 2016; Dadda et al., 2010). However, it is still largely unknown whether such laterality in sensory-behavior coupling evolves during adaptation to different environments.

A suitable evolutionary model for investigating this question is the teleost *Astyanax mexicanus*, which has evolved two forms, the blind cave dwelling form (cavefish) and the sighted surface dwelling form (surface fish) (Keene et al., 2015; Protas and Jeffery, 2012; Rétaux and Casane, 2013; Wilkens, 1988). Within the past few million years, at least 29 geographically isolated *Astyanax* cavefish populations were established by two or three radiations of the ancestral surface form, once the ancestors became isolated in the limestone caves of the Sierra de El Abra region in northeastern Mexico (Bradic et al., 2012; Coghill et al., 2014; Gross, 2012). Thereafter, some of these cavefish populations independently evolved troglomorphic traits (Borowsky, 2008; Mitchell et al., 1977; Ornelas-García et al., 2008; Strecker et al., 2012; Wilkens, 1988). Compared to surface fish, cavefish have smaller and subcutaneous eyes, less pigment, less calcified bone in both the cranium and in the whole body, loss of vertebrae, more teeth, larger jaws, more mechanosensory neuromasts, taste buds, fat tissue and enlarged olfactory epithelium (Jeffery, 2001; Keene et al., 2015; Wilkens, 1988).

An advantage of this system for investigating laterality is that cavefish are known to show laterality in the neuromast-sensory modality, i.e., cavefish are more likely to pass by a novel immobile object using their right side than their left, suggesting that they prefer to investigate novel objects with their right-side neuromasts (Perera and Braithwaite, 2005). This can be related to spatial learning (related

to Sovrano et al., 2005). However, it is unknown whether surface fish show laterality (i.e. ancestral state), and whether other behaviors also show laterality.

To address this, here we study another sensory-based behavior that is relatively easy to assay: an adaptive foraging behavior called vibration attraction behavior (VAB), where fish, when in darkness, are attracted to a vibrating object (Yoshizawa et al., 2010). For cavefish, VAB is significantly enhanced and advantageous because fish with higher VAB more efficiently capture prey in the dark (Yoshizawa et al., 2010). Furthermore, subsequent studies have shown that VAB is largely regulated by the cranial neuromasts at the eye-orbital region (Yoshizawa et al., 2012).

Here, we first investigated how the differences in neuromast development in surface fish and cavefish influence VAB, and, second, if laterality is involved in this adaptive sensory-behavior system. The development of neuromasts, which primarily detect the organism's acceleration and the water flow/velocity around amphibians and fish (Coombs et al., 2014), happens in two waves. In the first wave, they develop from the lateral line neural placodes and mainly differentiate into acceleration sensing-canal neuromasts. In the second wave, they develop from budding process of other neuromasts, where they mainly differentiate into superficial neuromasts (SN) (Webb, 2013). In surface and cavefish, the first wave of neuromast development is indistinguishable (Yoshizawa et al., 2010); however, the second wave mainly differs in that surface fish have fewer SN than cavefish after 2 months post fertilization (mpf) (Yoshizawa et al., 2010).

It is then possible that the difference in SN number between surface fish and cavefish is a result of differences in the bone formation underlying the SN budding site. Studies in zebrafish have shown that the bone formation underneath the site of SN budding determines budding location and timing; growth zone of dermal bone seems to encourage SN budding (Kimmel et al., 2003; Wada et al., 2010, 2008). Furthermore, these studies have also suggested that bone formation can be modified in both positive and

negative ways (depending on the bone and developmental timing) by endothelin signaling, such that endothelin acts as 'morphogen' (Kimmel et al., 2003).

To first determine whether differences in bone development underlie SN number, we administered antagonists of endothelin receptors (ET_A and ET_B) to both morphs of *A. mexicanus* before and during dermal suborbital bone development. One month of treatment induced more SN and bone, but VAB was not significantly differentiated. This inhibition of the endothelin signaling also revealed that the bone formation is not associated with the SN development at this developmental stage of *Astyanax mexicanus*. Lastly, to investigate if the adaptive neuromast-VAB system in cavefish operates with laterality, we assessed the study results through a correlation analysis. We revealed that the level of VAB is positively correlated with the number of left SN in cavefish but not with the number of right SN, bone asymmetries, or any of the traits in surface fish. Our study thus suggests that laterality in using the sensory system may have evolved in cavefish.

2. Materials and Methods

2.1. A. mexicanus *husbandry and ethics statement*

The *Astyanax mexicanus* surface population used in this study consisted of laboratory raised descendants of an original collection made in Balmorhea Springs State Park, Texas (USA). The cave population consisted of laboratory raised descendants of original collections from Cueva de El Pachón in Tamaulipas (México). Fish used in the assays ranged from 1 month to 7 months old and were raised in the lab within a glass specimen dish with a diameter and height of 89 and 39 mm, respectively (Pyrex dishes, VWR International, Radnor, PA, USA). Water volumes were adjusted according to the experiment between 150 to 250 ml. Each dish housed 15 to 20 fish until 4 months old, then fish were transferred to a plastic tray in dimensions of 15.7 × 15.7 × 7.6 cm (l × w × h) after the drug treatment. Fish were fed

living *Artemia salina* larvae twice per day for all experiments. All animal procedures were performed under the protocol 17-2560 approved by the Institutional Animal Care and Use Committee (IACUC) at University of Hawai‘i. Resource information is also available in Key Resources Table.

2.2. Inhibition of endothelin signaling

Approximately 15 of either cave and surface morph of 1 month old or 2 months old were placed under bath treatment either with phosphate buffered saline (PBS) only (0 nM; control), or with concentrations of 50 nM, 100 nM or 200 nM of the ET_A antagonist BQ-123 (Selleckchem, Houston, TX, USA) prepared with conditioned water (pH 6.8-7.0, Conductivity at 600-700 µS). This range of drug concentration (0 – 200 nM of BQ-123) was determined from a result of cell culture experiment (Ceccarelli et al., 2003). Treatments were performed for 1 or 2 months (Fig. 1). Treatments using PD145065 (non-selective ET_A/ET_B antagonist PD: MilliporeSigma, St. Louis, MO) were performed similarly at a concentration of 250 nM or 1 µM for 1 month. During these drug treatment experiments, drug solutions were replaced with fresh solutions every two days for 1 month or 2 months. The range of drug concentration was determined by referring to the former study (Ceccarelli et al., 2003). Known effects of ET antagonists are high blood pressure and hypertension (Filep et al., 1994); these antagonists potentially enhance nociception via dorsal root ganglia (Mule et al., 2017). We have not detected any hypertension or nociception related behavior during our experiment. Resource information is also available in Key Resources Table.

2.3 Vibration attraction behavior (VAB)

We assayed VAB as described previously (M. Yoshizawa et al., 2012a, 2012b, Yoshizawa et al., 2015, 2010). Briefly, individuals were acclimated in a cylindrical assay chamber (Pyrex 325 ml glass dish, 10 cm diameter 5 cm high, Corning, Corning, NY, USA) filled with conditioned water (pH 6.8-7.0;

conductivity approximately 600 μS) for 4–5 days prior to the assay. During testing, vibration stimuli was generated with a 7.5 mm-diameter glass rod vibrating at 40 Hz using a GW Instek SFG-1003 DDS Function Generator (Good Will Instrument Co., Ltd., New Taipei City, Taiwan) with an audio speaker (Pro Speakers, Apple, Cupertino, CA, USA). The number of approaches (NOA) to the vibrating rod was video recorded by using a customized Microsoft MAIN-31891 LifeCam Studio installed with a zoom lens (Zoom 7000, Navitar, Rochester, NY) and a virtualdub v1.10.4 video capture software (licensed under the GNU General Public License) during a three-minute period under infrared illumination (880 nm wave length, BL41192-880 black light, Advanced Illumination, Rochester, VT, USA); then, the number of approaches was counted using a tracker plugin of ImageJ v1.51o software (NIH, Bethesda, MD, USA).

The same individuals were measured twice: at 2 mpf and at 3-7 mpf for Exp-A and B; and at 3 mpf and at 4 mpf for Exp-C and D (Fig. 1A). Note that in VAB, a score of 2 or below the square root of the number of approaches is the random background level, and VAB was defined as >2 (Yoshizawa et al., 2010). In previous studies, VAB was not observed in cavefish at 2 mpf but was detectable after ≥3 mpf (Yoshizawa et al., 2010). Resource information is also available in Key Resources Table.

2.4 Vital bone and superficial neuromast imaging

Bone imaging: Fish were vitally stained with 0.01% calcein (MP Biomedicals, LLC, Santa Ana, CA, USA) in conditioned water (pH 6.8-7.0, conductivity 600-700 μS) overnight to visualize the calcified bones; then, counter-staining using 4-Di-1-ASP neuromast staining (see below) was performed. Both left and right sides of the fish cranium were imaged using a BX61WI upright fluorescent microscope equipped with 2.5 x MPlanFL N lens with a numerical aperture of 0.08, a FITC filter set (Olympus, Shinjuku, Japan) and an ORCA-Flash4.0 digital camera (Hamamatsu Photonics, Hamamatsu, Japan). The bone imaging was performed in Experiment-C and D. Under the fluorescent digital image, areas for 1st

suborbital bone (SO1), SO2, SO3, SO4 and SO5 were measured using a polygon selection function of ImageJ v1.51o software.

Neuromast imaging: Neuromast vital staining was performed as described previously (Jørgenson, 1989; Yoshizawa et al., 2010). Fish were immersed in 25 µg/ml 4-(4-(dimethylaminostyryl)-1-methylpyridinium iodide (4-Di-1-ASP; MilliporeSigma) dissolved in conditioned water for one hour, followed by anesthesia in ice-cold 66.7 µg/mml Ethyl 3-aminobenzoate methanesulfonate salt (MS222, MilliporeSigma) in conditioned water. Fish were then visualized under the same fluorescence microscope as used in bone imaging (BX61WI Olympus microscope with 2.5 x MPlanFL N lens, a Rhodamine filter set and an ORCA-Flash4.0 digital camera). Neuromasts were counted on digital images of 4-Di-1-ASP-stained fish using the "Analyze Particles" function of ImageJ software. Superficial neuromasts were counted both in the epidermis over the cranial third suborbital (SO3) bone and within the orbital epidermis dorsal to the line of the suborbital canal neuromast for both the left and right side (Figure 2).

The same individuals were imaged twice after VAB assay (also see section *2.3 Vibration attraction behavior (VAB)*). Resource information is also available in Key Resources Table.

2.5 Statistical Analysis

All statistical analyses, including the correlation analysis and two-way ANOVA, were performed in IBM SPSS 24.0.0.0 software (IBM, North Castle, NY, USA). We also used the Mann-Whitney non-parametric test under SPSS when sample sizes were significantly different, samples which violated the equality of variances and/or simple comparison of two groups were applicable.

To test whether the observed levels of Pearson correlation *r*-values are valid (Table S1), we performed bootstrapping using 10,000 random samplings of VAB level and the morphological trait of interest. From this random sampling, we calculated Studentized 95% confidence intervals of Pearson

correlation *r*. If these intervals did not include zero, we concluded that there was a 95% chance that the Pearson *r*-values were valid. We used *boot* and *boot.ci* function to calculate Studentized 95% confidence intervals in 'boot' package of R (Davison and Hinkley, 1997).

3. Results and Discussion

Our first goal was to determine whether altered bone formation affects SN development. According to Wada et al., endothelin plays a role in the bone development, and therefore neuromast development of early stage zebrafish larvae (~ 3 days post fertilization) (Wada et al., 2010); however, cavefish start to show significantly higher numbers of SN (compared to surface fish) much later on, between 1 and 2 months post-fertilization (mpf) (Yoshizawa et al., 2010). In addition, the dermal bone of cavefish at the suborbital region, where SN are enhanced, also begins to form at 2 months post-fertilization (mpf) (Yamamoto et al., 2003). Therefore, we first investigated the relationship between endothelin signaling and the development of the superficial neuromasts (SN) at 1-2 mpf (Experiment-A and B, or Exp-A and B: a period of SN enhancement), followed by studies to resolve the relationship between bone formation and the SN number at 2-3 mpf (Experiment-C and D, or Exp-C and D: a period of dermal bone development) (Fig. 1A).

In Exp-A and B, we further discriminated maturity and body growth. We reared fish in space constrained conditions (15 fish in 150 ml water: Exp-A, Fig. 1A) in comparison to the standard rearing condition (15 fish in 250 ml water: Exp-B, Fig. 1A). This spatial restriction slowed down the growth rate (Gallo and Jeffery, 2012) (Table S4) and was performed for 1 month during the drug treatment; then, standard rearing conditions (250 ml) were applied without drug after 2 mpf. Fish in the control (no-drug and either in 150 or 250 ml) conditions were also reared in a no-drug environment in 250 ml after 1 month of the drug treatment (Exp-B, Fig. 1A). After the drug treatment, we measured the vibration attraction behaviors (VAB) and the SN number at the 3rd suborbital bone region (SO3) at 2 mpf and over

3 mpf for Exp-A and B. Please note that the number of SN at the eye orbit, which has been found to be tightly associated with VAB in later stages (≥ 6 mpf), was very low and not correlated with VAB in fish as young as 4 mpf (see below and Table S1) (Yoshizawa et al., 2012).

In surface fish in Exp-A (with a 150 ml rearing environment), after the one month-drug treatment (2 mpf) and after subsequent rearing without drug (≥ 3 mpf), neither of the ET endothelin receptor antagonist (BQ-123—ET_A antagonist or PD145065—both ET_A and ET_B antagonist) in any concentration (50 nM – 1 μM) affected the SN number or the level of VAB compared to control surface fish (Fig. 1B and 1F). However, when comparing between the two time points, there was a significant increase in VAB and SN number from surface fish at 2 mpf to ≥3 mpf (Fig. 1B and 1F). This slight development of SN as fish age is consistent with a previous study, but the VAB enhancement is new (Yoshizawa et al., 2010). This age factor did not affect surface fish VAB in the 250 ml condition (Fig. 1H), which was consistent with the previous study (Yoshizawa et al., 2010); this age-enhanced VAB of surface fish in 150 ml indicates that the high-density rearing environment could enhance VAB in surface fish (Fig. 1F and 1H; 2mpf: Mann-Whitney U =3,581.0, Bonferroni corrected P = 0.856, N = 110 and 70 for the 150 and the 250 ml rearing condition, respectively; and ≥3 mpf: U = 886.5, Bonferroni corrected P = 0.0487, N = 33 and 81 for the 150 ml and 250 ml rearing condition). This may have been because fish reared under these conditions show more boldness (perhaps due to limited spatial resources), so that instead of avoiding a vibrating object, they ram it. Whatever the reason, the standard rearing conditions (250 ml body of water) did not induce VAB in surface fish (see below too) (Fig. 1H).

In cavefish in Exp-A, the ET_A antagonist, BQ-123, induced more SN when present in a concentration of 100 nM but not in 50 or 200 nM (Fig. 1C). As endothelin signaling is proposed to act as a morphogen for cranial bone formation—endothelin signaling can both induce and reduce bone formation depending on its concentration and the target bone (Kimmel et al., 2003)—the bell-shaped response in cavefish SN indeed supports that endothelin signaling acts as a morphogen by having threshold effect in their concentration (Fig. 1C). This effect was diminished after removing the drug (≥3

mpf, Fig. 1C). Although 2 mpf fish showed more SN in response to 100 nM BQ-123, and SN are a major sensor for VAB, VAB was not increased in 2 mpf (Fig. 1C and 1G) but did increase according with fish age (Fig. 1G).

Similar results to Exp-A were obtained in Exp-B, but Exp-B showed a more exaggerated drug effect. SN enhancement in both surface fish and cavefish was detected at 2 mpf when BQ-123 was present at 50 and 100 nM (Fig 1D and 1E). In cavefish, but not in surface fish, this enhancement lasted after the drug was removed (≥ 3 mpf, Fig. 1D, 1E). However, the SN enhancement was not sufficient to increase the VAB level in either surface fish or cavefish (Fig. 1H, 1I).

As in Exp-A, in Exp B the SN number did increase along with development (2 mpf vs ≥3 mpf) in both surface fish and cavefish, but numbers were higher for fish in the less crowded environment of Exp-B, suggesting that growth plays a major role for SN development. Note that the body sizes were larger in the 250 ml condition than in the 150 ml condition at ≥ 3 mpf. The growth represented by the lengths between the center of the anterior nostril and the corner made by the preopercular and mandibular canals was significantly greater in the 250 ml than the 150 ml rearing condition (Table S4). In contrast, VAB may not depend so much on growth but rather maturity, since the level of VAB in cavefish was indistinguishable between Exp-A and B for fish of comparable ages (Fig. 1G and 1I; 2 mpf: $U = 2{,}885.0$, $P = 0.074$, $N = 87$ and 79 for the 150 and the 250 ml rearing condition; and ≥ 3 mpf: $U = 1{,}994.5$, $P = 0.194$, $N = 38$ and 122 for the 150 and the 250 ml rearing condition; P-values were not adjusted for multiple comparisons).

Lastly, the non-selective ET_A/ET_B antagonist (PD145065) acted similarly to 200 nM BQ-123 and did not change the SN number or VAB in surface fish or cavefish (neither ANOVA nor post hoc tests showed any significant difference; Fig. 1 and Table S2). This may be due to strong inhibition of endothelin signaling by blocking both ET_A and ET_B.

Overall, for Exp-A and B we observed increased SN number in both surface fish and cavefish when inhibiting ET_A, but this sensory enhancement was not sufficient to increase the VAB level. Instead, the VAB level was influenced by maturity/age in cavefish (Fig. 1G and 1I) or crowdedness in surface fish (Fig. 1F and 1H).

Next, to determine the developmental relationship between SN number, suborbital bones and VAB, we inhibited ET_A signaling only, using BQ-123, at a later developmental stage; namely, when the earliest suborbital bone, the second suborbital bone (SO2), emerged (Exp-C for 1 month and Exp-D for 2 month treatments, Fig. 1A). Furthermore, because Gross et al. described that adult cavefish show an asymmetric distribution of SN and bone fragmentation between their left and right sides (Gross et al., 2016a, 2016b, 2014), we also investigated left-right symmetry of the SN number and suborbital bone areas under this BQ-123 treatment.

In Exp-C (1 month of BQ-123 treatment; fish tested at 3 mpf), surface fish displayed symmetry in the mean SN number and the mean area of suborbital bone (SO1-SO5) on the right and left sides (Fig. 2A-2M', and Fig. 3A-3C'). Interestingly, the older (4 mpf) non-drug treated (control) surface fish in Exp-D showed asymmetry in suborbital bone area, where the left suborbital bones were smaller than those on the right (SO1-SO4) (Fig. 2E', 2G' and 2I'). However, this left-right asymmetry was not detectable in the SN number (Fig. 2A') (Table S5), suggesting that bone and SN are regulated differently. In addition, surface fish treated with BQ-123 showed no detectable differences from the control surface fish in suborbital bone area or SN number at either 3 mpf (Exp-C) or 4 mpf (Exp-D) (Fig. 3A-3M', Table S5).

At the behavioral level in surface fish, there was no detectable difference in VAB based on either drug treatment (comparing drug-treated fish to controls) or age (comparing 4 mpf to 3 mpf fish) (Fig. 2Q).

Overall, for the surface fish, BQ-123 treatment did not change SN number and bone formation. However, we did see left-right suborbital bone asymmetry in surface fish at 4 mpf, even though adult surface fish establish left-right 'symmetry' in the cranial bones (Gross et al., 2016a, 2016b, 2014; Powers et al., 2017). This asymmetry in juvenile surface fish has also been observed by other research groups (Powers and Gross, personal communication), meaning that it must be adjusted by a developmental process before the fish becomes an adult. Nonetheless, the left-right asymmetry we observed in the surface fish suborbital bone did not correspond with asymmetry in SN number (Fig. 2A') or VAB level (Fig. 2Q)—SN number and VAB level stayed the same between Exp-C (left-right 'symmetry' in suborbital bones at 3 mpf) and Exp-D (left-right 'asymmetry' in suborbital bones at 4 mpf). Therefore, suborbital bone formation was not sufficient to change SN number or the VAB level in surface fish.

In cavefish, left-right asymmetry in suborbital bones was below the detection level in both Exp-C (3 mpf) and Exp-D (4 mpf) (but see P-values at SO1, SO2 and SO3 before Bonferroni correction; Table S5). Interestingly, left-right asymmetry in SN number was seen in younger stage cavefish (Exp-C, 3 mpf, Fig. 2B), but this SN asymmetry was not detectable in the older stage cavefish (Exp-D, 4 mpf, Fig. 2B'). In addition, cavefish treated with BQ-123 had much larger suborbital bone areas than surface fish (SO1 and SO2; Fig. 2C and 2C' vs 2D and 2D'; 2E and 2E' vs 2F and 2F') (Mean areas ± s.e.m. for SO1: 0.048 ± 0.002 and 0.074 ± 0.007 mm^2 for surface fish and cavefish, respectively; $t_{89.2} = -3.3$, $P = 0.002$. Mean areas for SO2: 0.204 ± 0.007 and 0.358 ± 0.022 mm^2 for surface fish and cavefish, $t_{88.7} = -6.6$, $P = 4.9 \times 10^{-9}$. P-values were adjusted by Bonferroni correction). Notably, the drug-induced enhancement of SO bone areas in cavefish was only observed on the right side (SO1 and SO3; Fig. 2D and 2H'). However, this bone enhancement was not associated with SN increase (Fig. 2B and 2B'), again supporting the conclusion in surface fish that bone formation is not associated with SN development.

In summary, treatment with endothelin antagonist BQ-123 did enlarge dermal bones in cavefish but not in surface fish. This result is likely to be associated with the initial stages of dermal bone formation because bone sizes of SO1 and SO3 in the cavefish control are much smaller than those of later

stages. In contrast, the suborbital bone sizes in the surface fish control were almost the same sizes as those of later stages. These growing bones in cavefish are artificially enlarged under drug treatment: Fig. 2D vs 2D', and 2H'). However, this dermal bone formation did not affect the SN development in either surface fish or cavefish.

Another notable observation was that cavefish suborbital bones had a slower ossification rate than those in surface fish (SO3-SO5; Fig. 2H', 2J' and 2L'), that is, the cavefish bones had larger areas but were not as thick as the bones of same-aged surface fish (cavefish had lighter calcein staining compared to surface fish, Fig. 3). This thin dermal bone may contribute to the elasticity of the cavefish skin surface, whereas in surface fish, the suborbital region is backed by a stiff bone plate. This elastic skin surface of cavefish may change the sensing property of SN, might yield better vibration sensing while cavefish swim.

As for cavefish behavior, the VAB level was not affected by BQ-123 treatment, but it was affected by age (Fig. 2R), consistent with the results of Exp-A and -B. Therefore, we did not detect any obvious link between morphological and behavioral traits. However, the highly variable VAB level observed here (relatively large standard error of means in Fig. 2R) may have masked a meaningful relationship. To visualize the association between VAB and each of the morphological traits in an individual, we performed a correlation analyses (Table S1).

Because VAB is more obvious at 4 mpf, we tested Exp-D data (see Fig. 1A too), which includes both control and drug treated individuals. We then first questioned whether the general increase of SN number or suborbital bone—not particularly any increases on the left or right sides—is associated with VAB level by using the sum of left-right morphological measurements.

Surface fish VAB was correlated with the sum of sizes for SO1, perhaps indicating that VAB is associated with growth. However, surface fish VAB showed no correlation with the left-right sum of SN

number (Exp-D) (Table S1). In contrast, cavefish VAB was not correlated with any summed morphological trait in all Exp-D individuals (Table S1). To further look at the effect of growth, we tested 3-4 mpf individuals in the control cavefish (non-drug treated) group. These individuals showed significant correlation between VAB level and each left-right summed morphological trait: SN number as well as areas of SO1, SO2, and the SO3 fragment (Table S1). Again, these correlations are likely associated with growth of the fish.

Next, we separately tested VAB correlations with individual left and right measurements. Surprisingly, for all cavefish individuals in Exp-D, including control and drug-treated fish, we detected a significant correlation between VAB level and the left SN number but not the right SN number (Table S1) (Fig. 4C and 4C'). We did not see any correlation between VAB level and the standard length of the fish, again indicating that variances in size (standard length and area of SOs) are not associated with VAB. In contrast to cavefish, surface fish VAB was not correlated with the SN number (right or left) but was correlated with the right SO1 area (Fig. 4B and 4B').

Since maturity is the factor that significantly increase VAB level (Fig. 2R), we next measured the correlation between VAB level and each morphological trait in the cavefish control group at 3 mpf and 4 mpf (Exp-C and Exp-D)(Table S1). We found a consistent and significant positive correlation between VAB and the left SN number. In addition, VAB was also positively correlated with the left SO1, SO2 and SO3 fragments, indicating that VAB level is associated with left-side traits: the higher the SN number and the larger SO1 and/or SO2 bone, the higher the VAB level becomes.

To determine whether relative asymmetry rather than absolute SN number on the left side is correlated with VAB in cavefish, we subtracted the SN number on the right from that on the left and tested the correlation for all cavefish data in Exp-D. The results again indicate that the asymmetry in SN number, where there are more SN on the left, correlate with VAB level (Pearson r = -0.364, Studentized 95% confidence interval: -0.651 ~ -0.133, P = 0.029), but VAB does not correlate with any other

asymmetries. Cavefish controls at 3-4 mpf also showed the same relationship, i.e., the SN number asymmetry was correlated with VAB (Pearson r = -0.503, 95% confidence interval: -0.812 ~ -0.275, P = 0.014); however, none of the morphological asymmetries in surface fish were correlated with VAB level (P > 0.05, Table S1).

In summary, for cavefish, the general increase in SN number was not correlated with VAB level, but the number of SN on their left side SN was significantly associated with VAB level. This association was not detected in surface fish in these developmental periods.

The laterality of brain and behavior is a longstanding research theme because laterality is seen so often in many ecological contexts (Bisazza et al., 1998; Rogers and Andrew, 2002; Sovrano et al., 1999; Vallortigara and Bisazza, 2002). Here, we first investigated the asymmetric association between an adaptive behavior and the left-right mechanosensory system in cavefish. Based on research by Wada et al., we started investigating the relationship between bone formation and SN development in the context of the endothelin molecular pathway. We found that the endothelin pathway regulates bone formation and the SN number differently, depending on developmental timing (earlier for SN and later for bone) and location (SN number was increased in the SO3 region, but suborbital bone was not formed at SO3 when SN appear), suggesting the independent regulation of SN and bone development at the suborbital region in this developmental stage (see Powers et al. in this issue too). Accordingly, although there was significant asymmetry in bone sizes and drug-accelerated bone formation in the suborbital region of surface fish and cavefish, this bone formation was not correlated with SN number or VAB level. Finally, we observed that in cavefish the number of SN on the left side is significantly correlated with VAB.

In following, we discuss the effect of growth on SN number and bone formation, and the evolution of laterality in cavefish

BQ-123 was able to increase the number of SN in cavefish but only slightly increase it in surface fish, indicating that cavefish SN show more sensitivity to endothelin signaling levels during development. This effect was enhanced in the standard rearing condition (250 ml) compared with the constrained condition (150 ml), suggesting that growth is an important factor for SN number.

This drug sensitivity in cavefish SN development may also contribute to the variation in morphological traits observed for cavefish, such as the left-right asymmetry in SN location and the shapes and sizes of cranial bones (Gross et al., 2016a; Powers et al., 2017). As we see more morphological variations in cave populations than in surface populations (Gross et al., 2016a, 2016b; Powers et al., 2017; Wilkens, 2010), it is interesting to consider the relationship between the loss of genetic variance and phenotypic variation. When animals experience a population bottleneck, i.e., significant reduction of genetic diversity due to the limited individuals, such as seen during cave colonization (Bradic et al., 2013, 2012), it is thought that they lose the genetic resources needed to generate phenotypic variation. However, these subpopulations often largely diversify their phenotypes to adapt to new environments, like caves (Culver, 1982; Culver and Pipan, 2009). This paradox—the observation of diversified phenotypes under reduced genetic resources—is explained by multiple but not exclusive theories: (1) The genetic variants are refilled by receiving multiple migrations from the original or different populations (Kolbe et al., 2004; Roman and Darling, 2007). (2) Hidden phenotypic variation is exposed by unmasking genetic diversity via reduced activity of chaperons, such as HSP90—called genetic assimilation (Jarosz and Lindquist, 2010; Rohner et al., 2013; Rutherford and Lindquist, 1998; Waddington, 1953). (3) Finally, animals may show developmental plasticity possibly through epigenetic modification (Bonduriansky and Day, 2009). In these regards, it would be interesting to investigate genome-phenome interactions in *A. mexicanus*.

We detected an asymmetric association between left-right SN number and VAB, where only the left SN number was correlated with the VAB level. However, the SN number itself was not distinguishable between the left and right sides (Fig. 2B'). Therefore, the correlation study assessed the phenotypes of each individual fish (instead of the grouped scores) in the control group and in the 50 nM and 100 nM BQ-123 treatment groups in Exp-D. Among these cavefish individuals, the ones that received relatively more sensory inputs from the left side (correlation resulted in "diff" in Table S1) and/or 'enough' inputs from the left (absolute SN number on the left; result of SN-L number in the top row of Table S1) expressed higher VAB. During routine swimming, cavefish do not show left-right preference (personal observation, and de Perera and Braithwaite, 2005), suggesting that this laterality is not seen without a particular stimulus. Future ablation studies, such as one-sided ablation of SN, should reveal the importance of left neuromasts for cavefish VAB.

In previous studies, SN ablation attenuated VAB, especially ablation at the eye-orbit region (Yoshizawa et al., 2012). However, our current study indicated that the number of SN is not associated with the VAB level. This discrepancy can be explained by hypothesizing that VAB is a combined result of the internal state (appetite, wakefulness, etc.) and sensory wiring. We have known that some individual surface fish show the intermediate level of VAB without enhancing SN (Yoshizawa et al., 2010). In addition, age/maturity (internal state development) rather than SN number was associated with the emergence of VAB (Fig. 1 and Fig. 2). Finally, it is reported that cavefish evolved an insatiable appetite (Aspiras et al., 2015). Among the cave populations of *A. mexicanus*, a point mutation in the melanocortin receptor 4 (*mc4r*) gene induces an insatiable appetite (Aspiras et al., 2015). This mutation may support VAB, in combination with the elaboration of the SN wiring to efficiently detect prey vibrating at 30-40 Hz (Yoshizawa et al., 2014, 2010). It will be interesting to test this hypothesis through tests of frequency responses and SN ablation study in the near future.

While *A. mexicanus* cavefish primarily use the left neuromasts for VAB, they use their right neuromasts to investigate 'still' novel objects (Perera and Braithwaite, 2005). We are not yet sure whether these lateralities are advantageous in dark cave ecosystems. Cavefish potentially evolved laterality in other behaviors such as startle response (Chivers et al., 2016; Dadda et al., 2010) because startle response also seems beneficial for avoiding cannibalistic attacks from cohorts, observed in laboratory conditions (personal observation). We can test the laterality in this behavior, and then we can also determine an advantage of laterality in these behaviors in the vision deprived environment.

As surface fish and cavefish are interfertile and can be used for powerful crossing experiments, *A. mexicanus* may serve as an attractive evolutionary genetic model for studying laterality in neural function and behavior.

Acknowledgement

We thank C. Valdez, C. Balaan, N. Cetraro, J. Choi, S. Fujita, K. Lactaoen, J. Nguyen, N. Simon, L. Tuttle and M. Worsham for support and maintaining the fish system and providing valuable inputs for this study; we thank M. Iwashita for critical reading. This work was supported by the Hawaii Community Foundation [grant number: 16CON-78919].

References

Aspiras, A.C., Rohner, N., Martineau, B., Borowsky, R.L., Tabin, C.J., 2015. Melanocortin 4 receptor mutations contribute to the adaptation of cavefish to nutrient-poor conditions. Proc. Natl. Acad. Sci. U. S. A. 112, 9668–9673.

Bisazza, A., Rogers, L.J., Vallortigara, G., 1998. The origins of cerebral asymmetry: a review of evidence of behavioural and brain lateralization in fishes, reptiles and amphibians. Neurosci. Biobehav. Rev. 22, 411–26.

Bonduriansky, R., Day, T., 2009. Nongenetic Inheritance and Its Evolutionary Implications. Annu. Rev. Ecol. Evol. Syst. 40, 103–125.

Borowsky, R., 2008. Restoring sight in blind cavefish. Curr. Biol. 18, R23–R24.

Bradic, M., Beerli, P., Garcia-de Leon, F.J., Esquivel-Bobadilla, S., Borowsky, R.L., 2012. Gene flow and population structure in the Mexican blind cavefish complex (*Astyanax mexicanus*). BMC Evol. Biol. 12, 9 doi:10.1186/1471-2148-12-9.

Bradic, M., Teotónio, H., Borowsky, R.L., 2013. The population genomics of repeated evolution in the blind cavefish *Astyanax mexicanus*. Mol. Biol. Evol. 30, 2383–400.

Ceccarelli, F., Scavuzzo, M.C., Giusti, L., Bigini, G., Costa, B., Carnicelli, V., Zucchi, R., Lucacchini, A., Mazzoni, M.R., 2003. ETAreceptor-mediated Ca2+mobilisation in H9c2 cardiac cells. Biochem. Pharmacol. 65, 783–793.

Chivers, D.P., McCormick, M.I., Allan, B.J.M., Mitchell, M.D., Gonçalves, E.J., Bryshun, R., Ferrari, M.C.O., 2016. At odds with the group: changes in lateralization and escape performance reveal conformity and conflict in fish schools. Proceedings. Biol. Sci. 283, 20161127.

Chivers, D.P., McCormick, M.I., Warren, D.T., Allan, B.J.M., Ramasamy, R.A., Arvizu, B.K., Glue, M., Ferrari, M.C.O., 2017. Competitive superiority versus predation savvy: the two sides of behavioural lateralization. Anim. Behav. 130, 9–15.

Coghill, L.M., Darrin Hulsey, C., Chaves-Campos, J., García de Leon, F.J., Johnson, S.G., 2014. Next generation phylogeography of cave and surface *Astyanax mexicanus*. Mol. Phylogenet. Evol. 79, 368–374.

Coombs, S., Bleckmann, H., Fay, R.R., Popper, A.N., 2014. The lateral line system. Springer, New York.

Culver, D.C., 1982. Cave life, evolution and ecology. Harvard University Press, Cambridge.

Culver, D.C., Pipan, T., 2009. The biology of caves and other subterranean habitats, The biology of habitats series. Oxford University Press, Oxford.

Dadda, M., Koolhaas, W.H., Domenici, P., 2010. Behavioural asymmetry affects escape performance in a teleost fish. Biol. Lett. 6, 414–7.

Davison, A.C., Hinkley, D. V., 1997. Bootstrap Methods and Their Applications. Cambridge University

Press, Cambridge.

de Perera, T.B., Braithwaite, V.A., 2005. Laterality in a non-visual sensory modality--the lateral line of fish. Curr. Biol. 15, R241–R242.

Filep, J.G., Clozel, M., Fournier, A., Fóldes-Filep, É., 1994. Characterization of receptors mediating vascular responses to endothelin-1 in the conscious rat. Br. J. Pharmacol. 113, 845–852.

Gallo, N.D., Jeffery, W.R., 2012. Evolution of space dependent growth in the teleost Astyanax mexicanus. PLoS One 7, e41443.

Gross, J.B., 2012. The complex origin of *Astyanax* cavefish. BMC Evol. Biol. 12, 105 doi:10.1186/1471-2148-12-105.

Gross, J.B., Gangidine, A., Powers, A.K., 2016a. Asymmetric facial bone fragmentation mirrors asymmetric distribution of cranial neuromasts in blind Mexican cavefish. Symmetry (Basel). 8.

Gross, J.B., Krutzler, A.J., Carlson, B.M., 2014. Complex craniofacial changes in blind cave-dwelling fish are mediated by genetically symmetric and asymmetric loci. Genetics 196, 1303–19.

Gross, J.B., Stahl, B.A., Powers, A.K., Carlson, B.M., 2016b. Natural bone fragmentation in the blind cave-dwelling fish, *Astyanax mexicanus* : candidate gene identification through integrative comparative genomics. Evol. Dev. 18, 7–18.

Jarosz, D.F., Lindquist, S., 2010. Hsp90 and environmental stress transform the adaptive value of natural genetic variation. Science 330, 1820–4.

Jeffery, W.R., 2001. Cavefish as a model system in evolutionary developmental biology. Dev. Biol. 231, 1–12.

Jørgenson, J.M., 1989. Evolution of octavolateralis sensory cells., in: The Mechanosensory Lateral Line: Neurobiology and Evolution. pp. 115–145.

Keene, A.C., Yoshizawa, M., McGaugh, S.E., 2015. Biology and Evolution of the Mexican Cavefish, Biology and Evolution of the Mexican Cavefish. Elsevier Inc., Amsterdam.

Kimmel, C.B., Ullmann, B., Walker, M., Miller, C.T., Crump, J.G., 2003. Endothelin 1-mediated regulation of pharyngeal bone development in zebrafish. Development 130, 1339–1351.

Kolbe, J., Glor, R.E., Schettino, L.R., Lara, A.C., Larson, A., Losos, J.B., 2004. Genetic variation increases during biological invasion by a Cuban lizard. Nature 231, 177–181.

Magat, M., Brown, C., 2009. Laterality enhances cognition in Australian parrots. Proc. R. Soc. B Biol. Sci. 276, 4155–4162.

Mitchell, R.W., Russell, W.H., Elliott, W.R., 1977. Mexican eyeless characin fishes, genus *Astyanax*: Environment, distribution, and evolution., Special pu. ed, Special publications the museum Texas Tech University. Texas Tech Press, Texas.

Mule, N.K., Singh, J.N., Shah, K.U., Gulati, A., Sharma, S.S., 2017. Endothelin-1 Decreases Excitability of the Dorsal Root Ganglion Neurons via ETB Receptor. Mol. Neurobiol. 1–14.

Ornelas-García, C.P., Domínguez-Domínguez, O., Doadrio, I., 2008. Evolutionary history of the fish genus *Astyanax* Baird & Girard (1854) (Actinopterygii, Characidae) in Mesoamerica reveals multiple morphological homoplasies. BMC Evol. Biol. 8, 340 doi:10.1186/1471-2148-8-340.

Perera, T.B. De, Braithwaite, V.A., 2005. Laterality in a sensory modality — the lateral line of fish. Curr. Biol. 15, 241–242.

Powers, A.K., Davis, E.M., Kaplan, S.A., Gross, J.B., 2017. Cranial asymmetry arises later in the life history of the blind Mexican cavefish, Astyanax mexicanus. PLoS One 12, e0177419.

Protas, M., Jeffery, W.R., 2012. Evolution and development in cave animals: from fish to crustaceans. Wiley Interdiscip. Rev. Dev. Biol. 1, 823–845.

Rétaux, S., Casane, D., 2013. Evolution of eye development in the darkness of caves: adaptation, drift, or both? Evodevo 4, 26.

Rogers, L.J., Andrew, R.J., 2002. Comparative Vertebrate Lateralization, Cambridge University Press. Cambridge University Press, Cambridge.

Rohner, N., Jarosz, D.F.D.F., Kowalko, J.E.J.E., Yoshizawa, M., Jeffery, W.R.W.R., Borowsky, R.L.R.L., Lindquist, S., Tabin, C.J.C.J., 2013. Cryptic variation in morphological evolution: HSP90 as a capacitor for loss of eyes in cavefish. Science (80-.). 342, 1372–1375.

Roman, J., Darling, J.A., 2007. Paradox lost : genetic diversity and the success of aquatic invasions 22.

Rutherford, S.L., Lindquist, S., 1998. Hsp90 as a capacitor for morphological evolution. Nature 396, 336–342.

Sovrano, V.A., Dadda, M., Bisazza, A., 2005. Lateralized fish perform better than nonlateralized fish in spatial reorientation tasks. Behav. Brain Res. 163, 122–7.

Sovrano, V.A., Rainoldi, C., Bisazza, A., Vallortigara, G., 1999. Roots of brain specializations: Preferential left-eye use during mirror- image inspection in six species of teleost fish. Behav. Brain Res. 106, 175–180.

Strecker, U., Hausdorf, B., Wilkens, H., 2012. Parallel speciation in *Astyanax* cave fish (Teleostei) in Northern Mexico. Mol. Phylogenet. Evol. 62, 62–70.

Vallortigara, G., Bisazza, A., 2002. How ancient is brain lateralization?, in: Rogers, L.J., Andrew, R. (Eds.), Comparative Vertebrate Lateralization. Cambridge University Press, Cambridge, pp. 9–69.

Wada, H., Ghysen, A., Satou, C., Higashijima, S.-I., Kawakami, K., Hamaguchi, S., Sakaizumi, M., 2010. Dermal morphogenesis controls lateral line patterning during postembryonic development of teleost fish. Dev. Biol. 340, 583–594.

Wada, H., Hamaguchi, S., Sakaizumi, M., 2008. Development of diverse lateral line patterns on the teleost caudal fin. Dev. Dyn. 237, 2889–2902.

Waddington, C.H., 1953. Genetic assimilation of an acquired character. Evolution (N. Y). 7, 118–126.

Webb, J.F., 2013. Morphological Diversity, Development, and Evolution of the Mechanosensory Lateral

Line System, in: Coombs, S., Bleckmann, H., Fay, R.R., Popper, A.N. (Eds.), The Lateral Line System. Springer Handbook of Auditory Research 48. Springer, New York, pp. 17–72.

Wilkens, H., 1988. Evolution and genetics of epigean and cave *Astyanax-fasciatus* (Characidae, Pisces) - Support for the neutral mutation theory, in: Hecht, M.K., Wallace, B. (Eds.), Evolutionary Biology. Plenum Publishing Corporation, New York, pp. 271–367.

Wilkens, H., 2010. Genes, modules and the evolution of cave fish. Heredity (Edinb). 105, 413–422.

Yamamoto, Y., Espinasa, L., Stock, D.W., Jeffery, W.R., 2003. Development and evolution of craniofacial patterning is mediated by eye-dependent and -independent processes in the cavefish *Astyanax*. Evol. Dev. 5, 435–446.

Yoshizawa, M., Ashida, G., Jeffery, W.R., 2012a. Parental genetic effects in a cavefish adaptive behavior explain disparity between nuclear and mitochondrial DNA. Evolution (N. Y). 66.

Yoshizawa, M., Gorički, S., Soares, D., Jeffery, W.R.W.R., Gorički, Š., Soares, D., Jeffery, W.R.W.R., 2010. Evolution of a behavioral shift mediated by superficial neuromasts helps cavefish find food in darkness. Curr. Biol. 20, 1631–1636.

Yoshizawa, M., Jeffery, W.R.W.R., Van Netten, S.S.M., McHenry, M.J.M., 2014. The sensitivity of lateral line receptors and their role in the behavior of Mexican blind cavefish (*Astyanax mexicanus*). J. Exp. Biol. 217, 886–895.

Yoshizawa, M., Robinson, B.G., Duboué, E.R., Masek, P., Jaggard, J.B., O'Quin, K.E., Borowsky, R.L., Jeffery, W.R., Keene, A.C., 2015. Distinct genetic architecture underlies the emergence of sleep loss and prey-seeking behavior in the Mexican cavefish. BMC Biol. 13.

Yoshizawa, M., Yamamoto, Y., O'Quin, K.E., Jeffery, W.R., 2012b. Evolution of an adaptive behavior and its sensory receptors promotes eye regression in blind cavefish. BMC Biol. 10.

Yoshizawa, M., Yamamoto, Y., O'Quin, K.E., Jeffery, W.R., Kelly, E.O., others, 2012. Evolution of an adaptive behavior and its sensory receptors promotes eye regression in blind cavefish. BMC Biol. 10, 108.

Figure 1. Spatial restriction during rearing and endothelin signaling regulate the number of superficial neuromasts. A. Experimental setup for Experiment-A (Exp-A): ~15 1-month post fertilization (mpf) juveniles were reared in a 150 ml arena and were treated with drugs until 2 mpf; Experiment-B (Exp-B): ~15 1 mpf juveniles were reared in a 250 ml arena and were treated with drugs

until 2 mpf; Experiment-C (Exp-C): ~15 2 mpf juveniles were reared in a 250 ml arena and were treated with drug until 3 mpf; Experiment-D (Exp-D): ~15 2 mpf juveniles were reared in a 250 ml arena and were treated with drug until 4 mpf. (B-E). The number of superficial neuromasts (SN) around the 3rd suborbital bone (SO3) area. (F-I). The square root of the number of approaches toward a vibrating glass rod at 40 Hz (i.e. vibration attraction behavior: VAB). Each measurement of surface fish reared in a 150 ml arena (B, F), cavefish reared in a 150 ml arena (C, G), surface fish reared in 250 ml arena (D, H), and cavefish reared in a 250 ml arena (E, I) are shown. Bars represent means ± standard error of means (s.e.m.). Each bar is color coded for the drug concentration shown on the right side of the panel A. *: $P < 0.05$, **: $P< 0.01$, and ***: $P< 0.001$. The Bonferroni-adjusted significant results of two-way ANOVA are shown in each panel (i.e. 'Age' with their P-values). The post hoc Dunnett *t*-test was performed against the control within each age. For example, in the panel C, at 2 mpf, the number of SN under the control treatment was compared with the SN number under the 50 nM, 100 nM and 200 nM of BQ-123 treatments, and the 250 nM and 1 μM of PD145056 treatments. Among these tests, only comparison between the control and the 100 nM treatment was significantly different, therefore, it is indicated with asterisks. Missing data points in Fig. 1B-I (for example, missed data for 200 nM BQ-123 and 1 μM PD145056 in Fig. 1B, C, F, G) were due to the drug vulnerability in young fish (Exp-A) or difficulty in acquiring enough experimental fish (Exp-B). All statistics are available in Supplemental Table S2 and S3.

Figure 2. Drug and age effects on left-right asymmetry of the number of superficial neuromasts (SN) and the areas of suborbital bones. (A-B') The number of superficial neuromasts around the SO3 region. (C-D') The area of SO1 (μm^2). (E-F') The area of SO2 (μm^2). (G-H') The area of SO3 (μm^2). (I-J') The area of SO4 (μm^2). (K-L') the area of SO5 (μm^2). (M-N') The area of the largest fragment bone of SO3 (μm^2). (O-O') The area of the 2nd largest fragment bone of SO3 (μm^2). (P-P') The area of the 3rd largest fragment bone of SO3 (μm^2). See Figure 3 for the bone and SN locations. (Q, R) Square-rooted number of approaches. X-axis indicates drug concentration (0, 50 and 100 nM). Surface fish's morphological traits are in A, A', C, C', E, E', G, G', I, I', K, K', M and M', where the left column

indicates Exp-C (3 mpf) and right column indicates Exp-D (4 mpf). Cavefish's morphological traits are in B, B', D, D', F, F', H, H', J, J', L, L', N, N', O, O', P and P', where the left column indicates Exp-C (3 mpf) and right column indicates Exp-D (4 mpf). Bars represent means ± standard error of means. Each bar is color coded as left: red and right: green as shown in panel A. The numbers on the bars indicate N used for the analysis. *: $P < 0.05$, **: $P< 0.01$, and ***: $P< 0.001$. The Bonferroni-adjusted significant results of two-way ANOVA are shown in each panel (i.e. "Treatment" or "Left-Right" with their P-values). The post hoc Dunnett *t*-test was performed against the control for each side (left or right). For example, in the panel H', the right SO3 area under the control treatment was compared with the right SO areas under the 50 nM and 100 nM treatments. Among these two tests, only comparison between the control and the 100 nM treatment was significantly different, therefore, it is indicated with asterisks. All statistics are available in Supplemental Table S5.

Figure 3. Bone and superficial neuromast development at 3 month and 4 month old in Experiment-C and D . (A-F') Left and right side of surface fish images show SN staining (yellow dots, by 4-Di-1-ASP) and bone staining (blue, by calcein) for different BQ-123 treatments (0, 50 and 100 nM). Suborbital bones are outlined with white dots. (G-L') Left and right side of cavefish images show SN staining and bone staining in different BQ-123 treatments: 0, 50 and 100 nM. A-C' and G-K' show represented individuals for Exp-C, and D-F' and H-L' show individuals for Exp-D. The SO1-5 areas and SN numbers that were counted are shown in D. Scale of the images are the same and a scale bar at panel K indicates 1.0 mm.

Figure 4. Scatter plots for the SN number or the first suborbital bone (SO1) area against VAB (results in Exp-D). (A-B') Scatter plots of surface fish traits for the left and right SN number (A and A') and SO1 area (B and B') against the square-rooted number of approaches (VAB level). (C-D') Scatter

plots of cavefish traits for the left or right SN number (C and C') and SO1 area (D and D') against the square-rooted number of approaches (VAB level). Regression lines are shown on each panel. See also Table S1.

Highlights

- Endothelin signaling independently affects bone and neuromasts
- Endothelin signaling affects the development of neuromasts earlier and bone later
- Induced neuromasts did not affect VAB
- The number of left-side but not right-side neuromasts positively correlated with VAB

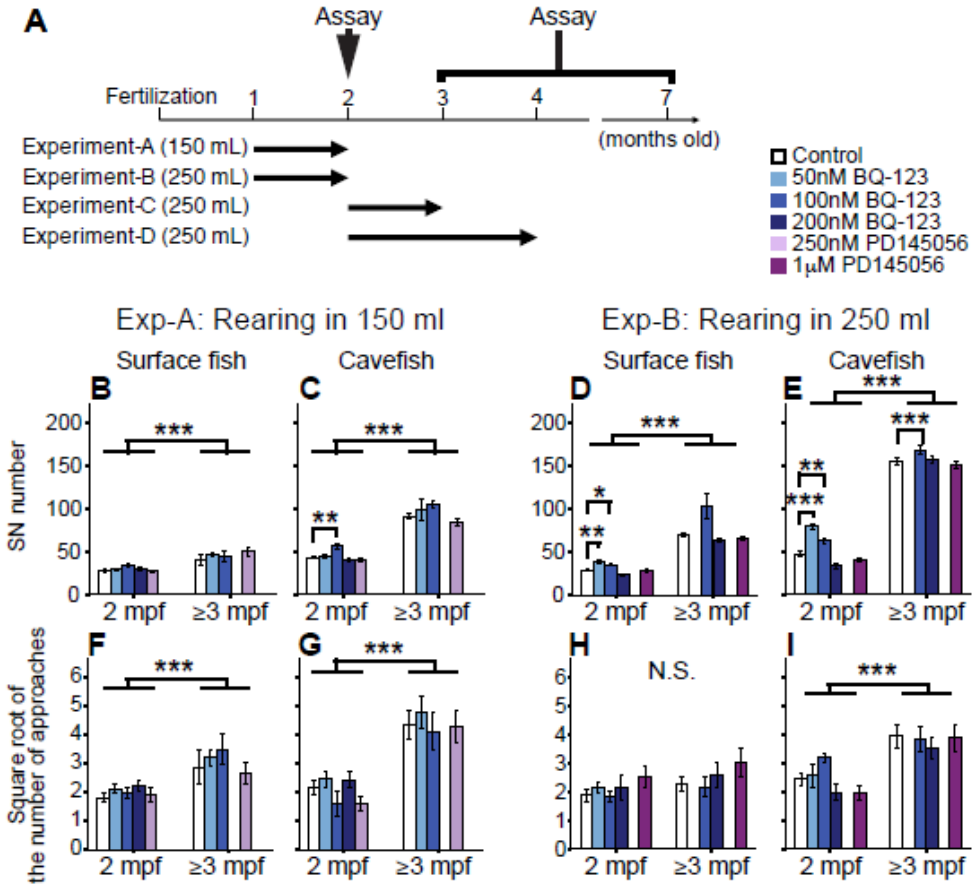

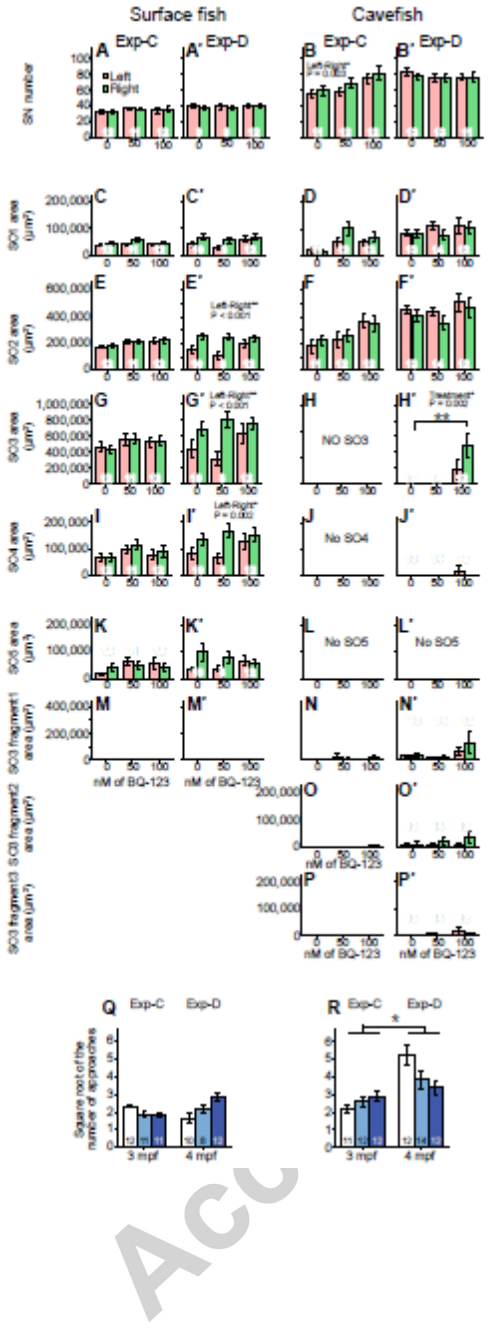

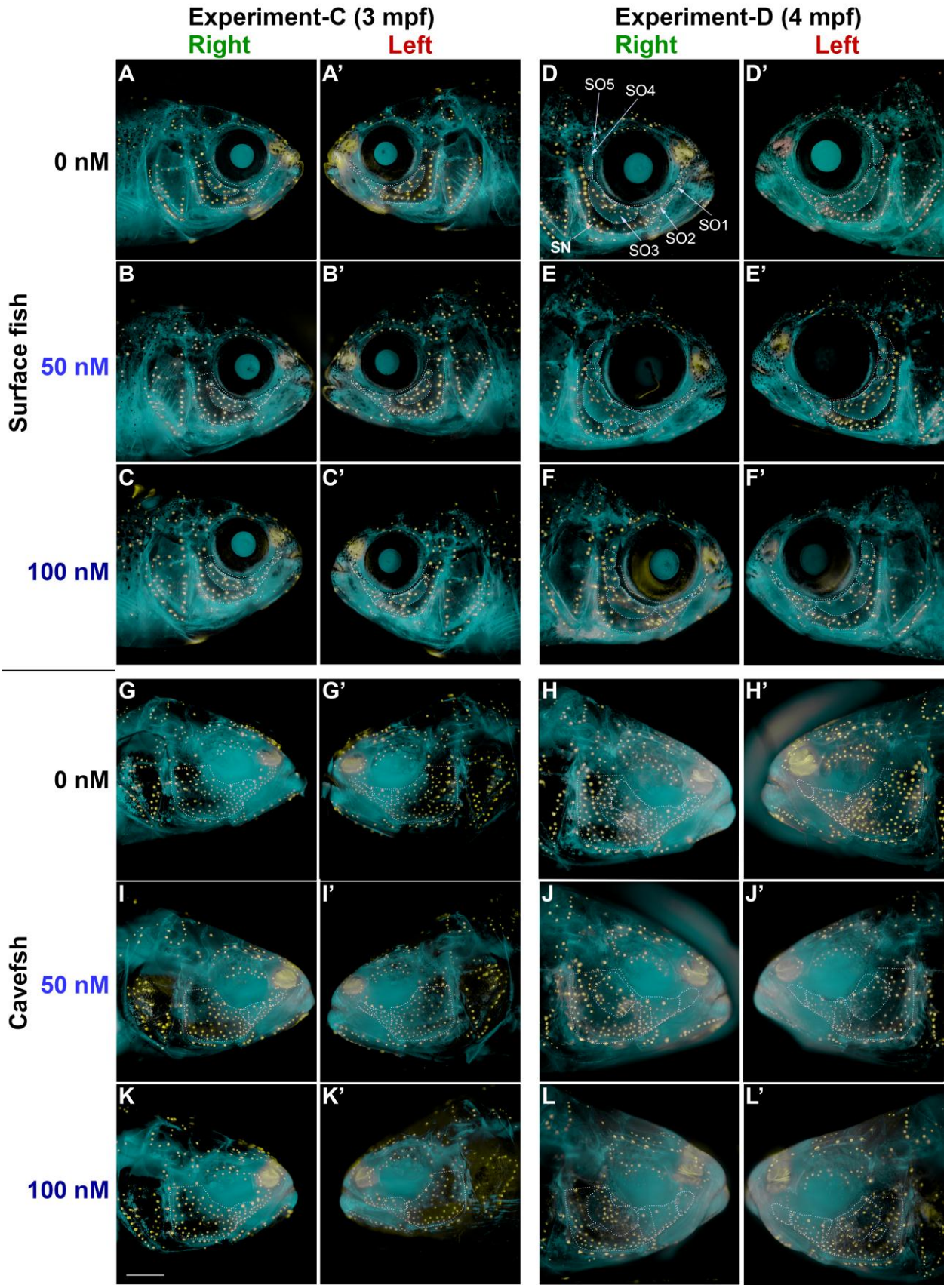
Experiment-C (3 mpf)
Right
Left
Experiment-D (4 mpf)
Right
Left
Surface fish
Cavefsh
0 nM
50 nM
100 nM
A
A'
B
B'
C
C'
D
D'
E
E'
F
F'
G
G'
H
H'
I
I'
J
J'
K
K'
L
L'
SO5
SO4
SO1
SO2
SO3
SN